Journal of Molecular Liquids 381 (2023) 121825

Contents lists available at ScienceDirect

Journal of Molecular Liquids

journal homepage: www.elsevier.com/locate/molliq

Self-assembly of bent-core amphiphiles joining the ethylene-oxide/lithium ion tandem

Martín Castillo-Vallés [a], César L. Folcia [b], Josu Ortega [b], Jesús Etxebarria [b], M. Blanca Ros [a,*]

[a] Instituto de Nanociencia y Materiales de Aragón (INMA), Departamento de Química Orgánica-Facultad de Ciencias, Universidad de Zaragoza-CSIC, E-50009 Zaragoza, Spain
[b] Department of Physics, Faculty of Science and Technology, UPV/EHU, E-48080 Bilbao, Spain

ARTICLE INFO

Keywords:
Amphiphile
Ethylene oxide
Lithium ion-complexes
Bent-core liquid crystals
Gels
Functional supramolecular materials

ABSTRACT

The synthesis, supramolecular self-assembly and structural characterization of a new family of tetraethylene oxide (TEG)-based bent-core compounds and their 1/1 lithium-containing complexes are reported. TEG-based bent-core amphiphiles, even joining the TEG/Li^+ tandem, are suitable building-blocks to achieve supramolecular nanostructures, in some cases showing chiral features from achiral molecules either in the mesophase or in solvents. The thermal and liquid crystal behavior of these materials studied by polarizing optical microscopy and X-ray diffraction confirmed that Li-based materials stabilized polar smectic C and helical nanofilament-type mesophases, in contrast to the non-liquid crystalline pure TEG-compounds. Alternatively, both the pure amphiphiles and the lithium-doped materials self-assemble into physical gels in non-polar solvents, displaying three-dimensional networks composed of long fibers with lamellar molecular organizations as shown by transmission electron microscopy and X-ray diffraction. Interestingly, biphenyl- and azobenzene-based bent core amphiphiles aggregate in solvent into chiral nanostructured morphologies with supramolecular trends comparable to their molecular arrangement in their liquid crystalline phases.

1. Introduction

The poly-ethylene oxide structures gather a wide range of characteristics that make them ubiquitous in the aim to new material development. In addition to the innate chemical properties such as flexibility, polarity or broad possibilities for supramolecular chemistry, they are commercially available in a varied offer of chain lengths or chemical functionalization. As a consequence, to think about poly-ethylene oxide (EO- or EG)-decorated compounds is a common and successful strategy in the route to novel advanced materials for very miscellaneous purposes, [1–9] in particular, for the design of molecular structures toward innovative soft materials for hydration/dehydration abilities, [2,6–7,10] ion conductive/transport pathways, [3,11–22] as well as for biocompatible and biodegradable amphiphiles. [23–27] Furthermore, segregation of chemically incompatible fragments of a molecule is a well-known driving force for the generation of nanostructured supramolecular systems. Thus building-blocks such as EO structures are present from block-molecules [28–31] to liquid crystals in bulk, [1,3,11,32–38] from aggregates to gels in solvents, [9,16,39–40] or from Langmuir-Blodgett films to Layer-by-Layer systems onto surfaces. [41–42].

Focused on EO-decorated liquid crystals, they have created high expectations for generation of new electrolytes, separation membranes, sensors or actuators by using 1D, 2D and 3D nanostructured classic, columnar, smectic and bicontinuous cubic mesophases respectively, and the manipulation of their orientation. [1,3,5,11,33–37] But interestingly, molecular interaction criteria for mesophase formation hardly differ from the features that define some attractive supramolecular systems and nanomaterials in bottom-up approaches. Thus, although really very little explored, [43] a variety of supramolecular assemblies have been reported by using molecules that form mesophases, i.e. mesogens, opening versatility and new potential for these supramolecular building-blocks in the route to functional supramolecular systems.

The molecular shape, intermolecular interactions and nanosegregation of the molecular moieties influence the self-assembly towards liquid-crystalline nanostructures. In this sense, since 1996, the emergence of the *bent-core liquid crystals* (BCLCs) [44–50] has certainly renewed the mesogen outlooks beyond classic calamitic or discotic mesophases. The distinctive angular shape of BC mesogens has been recognized to induce, apart from common mesophases, also other less

* Corresponding author.
E-mail address: bros@unizar.es (M. Blanca Ros).

https://doi.org/10.1016/j.molliq.2023.121825
Received 29 December 2022; Received in revised form 12 March 2023; Accepted 5 April 2023
Available online 11 April 2023
0167-7322/© 2023 The Author(s). Published by Elsevier B.V. This is an open access article under the CC BY-NC license (http://creativecommons.org/licenses/by-nc/4.0/).

conventional and interesting ones. Thus, elusive phases such as the *biaxial nematic phase* (N_B), [51–54] switchable *polar nematic* materials [55] or the highly interesting *twist-bend modulated nematic phase* (N_{TB}) [54,56–57] have been obtained from BC nematogens.

The BC molecules usually form smectic layers and adopt compact packing in the bend direction to restrict the rotation of the molecules along the long axis. Thus, a wide range of lamellar liquid crystal organizations showing spontaneous polarizations parallel to the layers have been described so far. Furthermore, the molecular tilt in some of these phases allows the layers to be chiral, despite the constituents having an achiral molecular nature. [48,50,58–60] These features have been the cornerstone of BCLC potential for applications. In addition to electrooptic-based display proposals, [50] further innovative functional abilities have been suggested for BCLC based on their ferro-, piezo-, pyroelectric, nonlinear optical, fluorescence, photoconductivity or magnetic responses. [50,61–65].

More recently, the *Helical Nano-Filament* (HNF) liquid crystalline morphologies [66–74] induced by these compounds have been studied to explore new alternatives for photovoltaics, chiral separation, surface control, several templating proposals or circular polarized luminescence goals. [75–80] From the perspective of polarity and the latest trends in supramolecular chirality, challenges such as the formation of helical superstructures, chirality amplification or the spontaneous breaking of mirror symmetry [59,81–83] look at BC mesophases, underlining opportunities in the context of chiral nanoarchitectonics. [84].

Interestingly, EO-based BC mesogens point to significant decrease of transition temperatures, [85–86]) abilities to form Langmuir-Blodgett films [87] or promising potential to aggregate in solvent, [88] but the examples reported so far are scarce. [43] Thus herein, we describe the synthesis and self-assembly properties of a novel family of EO-based BC compounds labelled as **TEG-Bx-0-14** (Scheme 1). All of them consist of a well-defined asymmetric structure, bearing a 5-ring BC structure (Bx). A 14-carbon atom aliphatic chain is incorporated at one end, and a hydrophilic tetraethylene oxide chain (TEG) is directly grafted at the other end, adding solubility and flexibility to induce nanophase separation. Three different connections have been considered for the lateral cores of the BC structures: a common ester linking group (B1) (compound **TEG-B1-0-14**, broadly used in our previous studies; [48,86]), the straight union *via* a biphenyl (Bi) moiety, inspired by the trend of biphenyl lateral cores to promote the HNFs mesophase formation [67,73,89] (compound **TEG-Bi-0-14**); and an azo linker (Bazo) (compound **TEG-Bazo-0-14**) in order to obtain photoresponsive materials. [90-91] Furthermore, considering the highly probed functional potential of the EO / cation tandem [3,15,17–18] hybrid materials have been prepared by complexing these BC-amphiphiles with lithium triflate (LiTF) in a 1/1 M ratio (complexes **Li-TEG-B1-0-14, Li-TEG-Bi-0-14** and **Li-TEG-Bazo-0-14** respectively).

The thermal and mesomorphic behaviour of these materials show that lithium-based materials **Li-TEG-Bx-0-14** stabilise lamellar mesomorphic behaviour, including chiral nanostructures similar to the helical nanofilaments described for the HNFs phase, [48,50,59] joining these mesophases to the stimulating ionic liquid crystal family, [38] while the pure compounds **TEG-Bx-0-14** melt to the isotropic liquid on heating and crystallize directly from the isotropic melt on cooling. Alternatively, to explore the supramolecular abilities of these materials, physical gels have been also prepared and characterized, showing that both, **TEG-Bx-0-14** and **Li-TEG-Bx-0-14** compounds, are able to form gels in non-polar solvents by the self-assembly into fibrillar morphologies with lamellar molecular organisations comparable to the molecular arrangement in mesophase. Thus, these TEG-based BC amphiphiles, even joining the TEG/Li^+ tandem, are suitable building-blocks to achieve highly demanded supramolecular nanostructured materials, i.e. fibers, soft-nanotubes or supramolecular gels, [92–94] in some cases showing chiral features both in the mesophase and in solvents.

2. Results

2.1. Synthesis of the ethylene oxide-based bent-core amphiphiles and their lithium-complexes

The synthesis of compounds **TEG-Bx-0-14** and lithium complexes **Li-TEG-Bx-0-14** were carried out through the synthetic routes shown in Schemes S1-S3 and adapted methods from similar intermediateś procedures. All experimental details and structural characterization of the compounds are described in the Supporting Information. Since all the **TEG-Bx-0-14** compounds show a common lateral structure grafted to the tetraethylene oxide chain (TEG), they were obtained *via* a convergent synthesis in which the same intermediate, a TEG-containg phenol, was coupled to three different carboxylic acids through a Steglich esterification. Bent-core compounds, **TEG-B1-0-14**, **TEG-Bi-0-14** and **TEG-Bazo-0-14,** were characterized by ^{1}H NMR, ^{13}C NMR, FTIR, mass spectrometry and elemental analysis to confirm the correct synthesis of the compounds.

The lithium-doped materials, named as **Li-TEG-B1-0-14, Li-TEG-Bi-0-14** and **Li-TEG-Bazo-0-14,** were prepared by mixing the ethylene oxide-based BC molecules with lithium triflate in a 1/1 M ratio, to ensure the average of four EO repetitive units per one Li cation. A downfield shifting of the –CH_2-O– signals was observed in the ^{1}H NMR spectra of the doped materials in comparison to the TEG-bent-core compounds (**Figure S5**). This was associated to the interaction between the EO chains with the cationic ion, either by intramolecular chelation or by linking neighbour molecules. On the other hand, the signals corresponding to the rigid BC structure and the aliphatic chain remained unaltered.

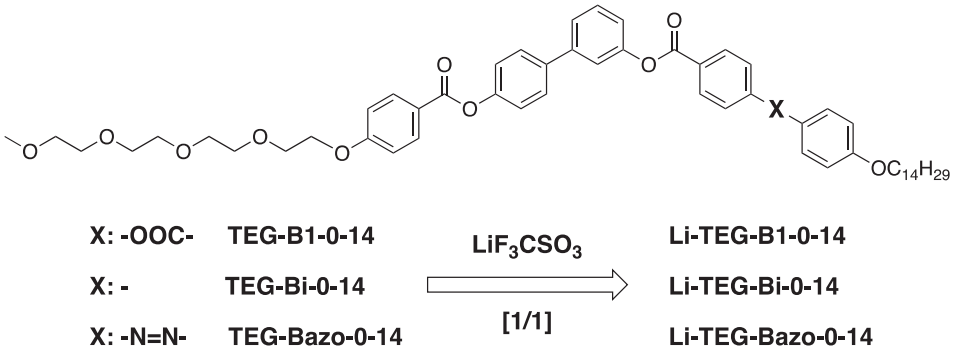

Scheme 1. Chemical structure and nomenclature of the three new tetraethylene oxide (TEG)-based bent-core compounds and their [1/1] lithium-complexes here reported.

2.2. Self-assembly processes

2.2.1. Liquid crystal self-assembly of bent-core amphiphiles

The thermal and mesomorphic behaviour of all the compounds and complexes were studied by polarized optical microscope (POM), thermogravimetric analysis (TGA), differential scanning calorimetry (DSC), and X-ray diffraction (XRD) experiments. All these data are gathered in Table 1. TGA experiments confirmed for all compounds and Li-complexes that the degradation temperatures with weight loss occurred at temperatures much higher than the transition to isotropic liquid, thus confirming the thermal stability of all the materials.

POM and DSC traces of all the compounds **TEG-Bx-0-14** only showed one phase transition associated to the direct melting to the isotropic liquid from the crystal state, and a direct crystallization on cooling, revealing that none of these compounds form liquid crystalline self-assemblies. On the contrary, all the Li-doped materials were able to induce stable mesophases, as observed by POM and DSC (Fig. 1**, S6** and **S7**). On cooling from the isotropic liquid, **Li-TEG-B1-0-14** entered into a mesophase around 90 °C showing a *schlieren* texture, that was unalterable until 60 °C. Below this temperature, the material crystallizes. In the case of **Li-TEG-Bi-0-14** and **Li-TEG-Bazo-0-14**, a single-phase transition was observed in DSC traces below the isotropic liquid at 98 and 90 °C, respectively. In both cases, POM observations confirmed the formation of a birefringent yet fluid liquid crystalline state, and textures were identified with others previously reported (Fig. 1 and **S6**). [67,73] The mesophase was stable at room temperature for **Li-TEG-Bi-0-14**.

It can be noticed that while melting temperatures of compounds **TEG-Bx-0-14** are close to those of the non-amphiphilic parent BC-molecules, [48] the EO chains disrupt the stabilization of mesophases. On the other hand, the presence of lithium atoms in **Li-TEG-Bx-0-14** samples seems to decrease the crystallization temperature and favours the formation of the molecular liquid crystalline order. As can be seen, the enthalpy changes for the isotropic-to-crystal transitions are larger than the values for the isotropic-to-mesophase ones evaluated for these Li-doped materials, supporting the existence of more disordered states in these hybrid materials (Table 1 and **Figure S7**).

XRD experiments at different temperatures of compounds **TEG-Bx-0-14** and hybrid materials **Li-TEG-Bx-0-14** confirmed a non-liquid crystalline nature for the former (**Figure S8**) and the existence of mesophases for the latter (Fig. 2 and **S9**).

In all the cases, the x-ray diagrams showed three reflections in the small angle region that were associated to a lamellar packing of the molecules both in the mesophase of the Li-doped materials and in the crystalline state of the pure materials. As an example, Fig. 2 shows the results obtained for both **TEG-B1-0-14**-based materials. These data confirm the strong tendency of these BC-based materials to self-organise in layers. In all the cases, the lamellar periodicities detected for the Li-doped materials **Li-TEG-Bx-0-14** are larger than for pure **TEG-Bx-0-14** compounds. This suggests that the lithium cations are intercalated within the ethylene oxide chains and this expands the lamellar arrangement.

Moving on to the assignation of the liquid crystalline organisation of complexes **Li-TEG-Bx-0-14**, the XRD pattern of **Li-TEG-B1-0-14** in the mesophase showed three intense and harmonic peaks in the small angle region that were assigned to (001), (002) and (003) reflections respectively, together with a diffuse halo in the wide-angle region (Fig. 2). With these results, the SmCP organisation can be proposed, commonly observed in BC molecular packing. [48,50] The layer spacing in this mesophase varied with the temperature, from 87.1 Å at 80 °C, 82.2 Å at 70 °C in the cooling process. Finally, at 60 °C the material crystallizes, and some additional reflections appear in the middle angle region and next to the diffuse halo (**Figure S9**).

Fig. 2 also shows the diffraction pattern of **Li-TEG-Bi-0-14** obtained on cooling from the isotropic liquid. In this case, patterns were identical in all the range of temperatures below the isotropic liquid down to room temperature. The diffractogram showed three harmonic peaks in the small angle region, assigned to (001), (002) and (003) reflections respectively, that correspond to a lamellar arrangement with a layer spacing of 91.8 Å. In the wide-angle region, the alkyl-chain disorder gives rise to a diffuse halo. However, some other sharper peaks corresponding to (hk0) reflections also appear superimposed to the halo. This peak organisation at low and wide angles is associated to the formation of a HNF-like mesophase, [50,73] in which the molecules are distributed within the layers with hexatic in-plane order. These results reinforce the hypothesis already mentioned by us that the incorporation of a biphenyl moiety in the lateral core of the bent-core molecule greatly favours the formation of a chiral HNF-type organisations. [67,73 89] The rigid nature of the biphenyl system seems to cause a strong tension between the two lateral parts of the bent-core system within the lamellas that is released through the twisting of the layers, giving rise to the helical nanofilaments characteristic of this mesophase. [66–67] Even though the mesophase for this material can be kept at room temperatures for some weeks, XRD experiments showed the appearance of some extra peaks in the middle angle range that correspond to the formation of a 3D crystal, thus confirming the crystallization of the sample over time.

Finally, XRD studies of **Li-TEG-Bazo-0-14** revealed the formation of a lamellar arrangement according to the harmonic peaks observed in the small angle region (**Figure S9**). Three maxima assigned to (001), (002) and (003) reflections respectively were observed. These peaks provided a layer spacing of 107.9 Å. In the wide-angle region, a diffuse halo was observed, together with a structure similar to that reported for **Li-TEG-Bi-0-14**. Consequently, the formation of an HNF-type mesophase is again proposed for **Li-TEG-Bazo-0-14**. However, in this case, an additional small peak in the small angle region that does not correspond to a periodic order was detected. This reflection showed an intensity that varied depending on the area of the sample irradiated with the x-ray beam and was placed between the (002) and the (003) peaks. It was assigned to a crystalline state that coexists in a small proportion with the mesophase.

In summary, all the Li-doped materials present locally a liquid crystalline lamellar structure. Moreover, in all the cases the layer spacings (82.2 Å for **Li-TEG-B1-0-14,** 91.8 Å for **Li-TEG-Bi-0-14,** and 107.9 Å for **Li-TEG-Bazo-0-14**) are larger than the estimated lengths of the EO-based bent-core amphiphiles (63.0 Å for **TEG-B1-0-14** and **TEG-Bazo-0-14,** and 60.5 Å for **TEG-Bi-0-14**), but smaller than twice this value. This suggests the formation of bilayer structures together with a partial intercalation of the flexible chains, and/or a tilt of the bent-core units. A close sight into the electronic density maps calculated from the XRD patterns as explained in the SI [95] reveals three differentiated regions (Fig. 3 and **S10**): a series of maxima related to the aromatic BC systems, a series of local minima associated to the EO chains, and a series of global minima assigned to the alkyl chains. According to this, each fraction of the molecule can form segregated sublayers, being the

Table 1
Phase transition temperatures, liquid-crystalline behaviour and degradation temperatures of the TEG-based bent-core compounds and the lithium-doped materials.

Compound	Phase transitions °C (kJ/mol) [a]	Degradation °C [b]
TEG-B1-0-14	Cr 74 (53.1) I / I 67 (52.6) Cr	267
TEG-Bi-0-14	Cr 102 (56.2) I / I 68 (56.2) Cr	346
TEG-Bazo-0-14	Cr 92 (55.3) I / I 89 (61.1) Cr	325
Li-TEG-B1-0-14	Cr 81 (14.9) SmCP 100 * (1.1) I / I 92 * (2.0) SmCP 60 (15.9) Cr	261
Li-TEG-Bi-0-14	Cr - HNF 99 * (36.5) I / I 98 (30.9) HNF	319
Li-TEG-Bazo-0-14	Cr + HNF 96 (32.5) I / I 90 (34.0) HNF + Cr	324

a) Data determined by DSC. Temperatures at the onset or (*) maximum of the peaks from second heating and cooling cycles at a scanning rate of 10 °C min^{-1}. Cr: crystal phase, SmCP: smectic C polar mesophase, HNF: helical nanofilament-type mesophase I: Isotropic liquid. b) Data determined by TGA. 2% mass loss temperature.

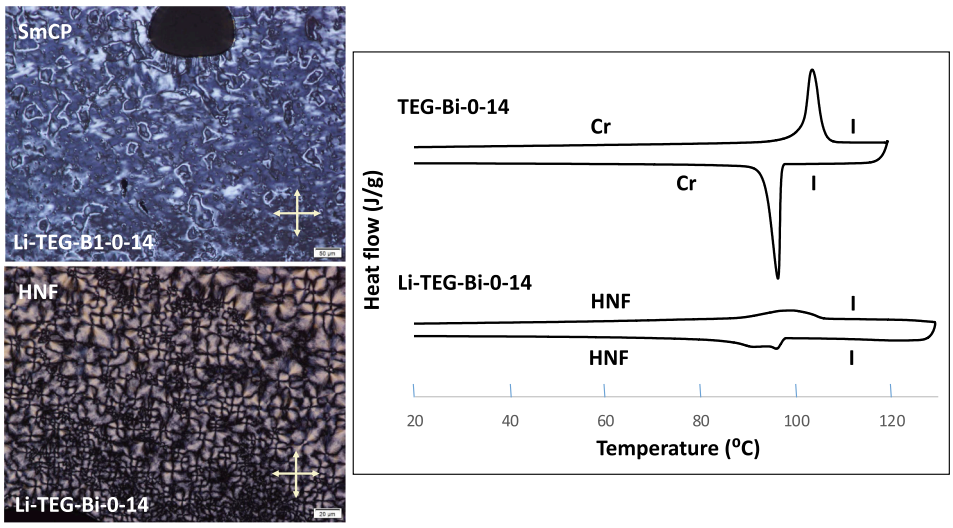

Fig. 1. (left) POM mesophase textures of **Li-TEG-B1-0-14** at 80 °C and of **Li-TEG-Bi-0-14** at 94 °C, obtained on cooling. (right) Comparative DSC thermograms of compound **TEG-Bi-0-14** and complex **Li-TEG-Bi-0-14**. Second heating/cooling cycles at a scanning rate of 10 °C min^{-1}.

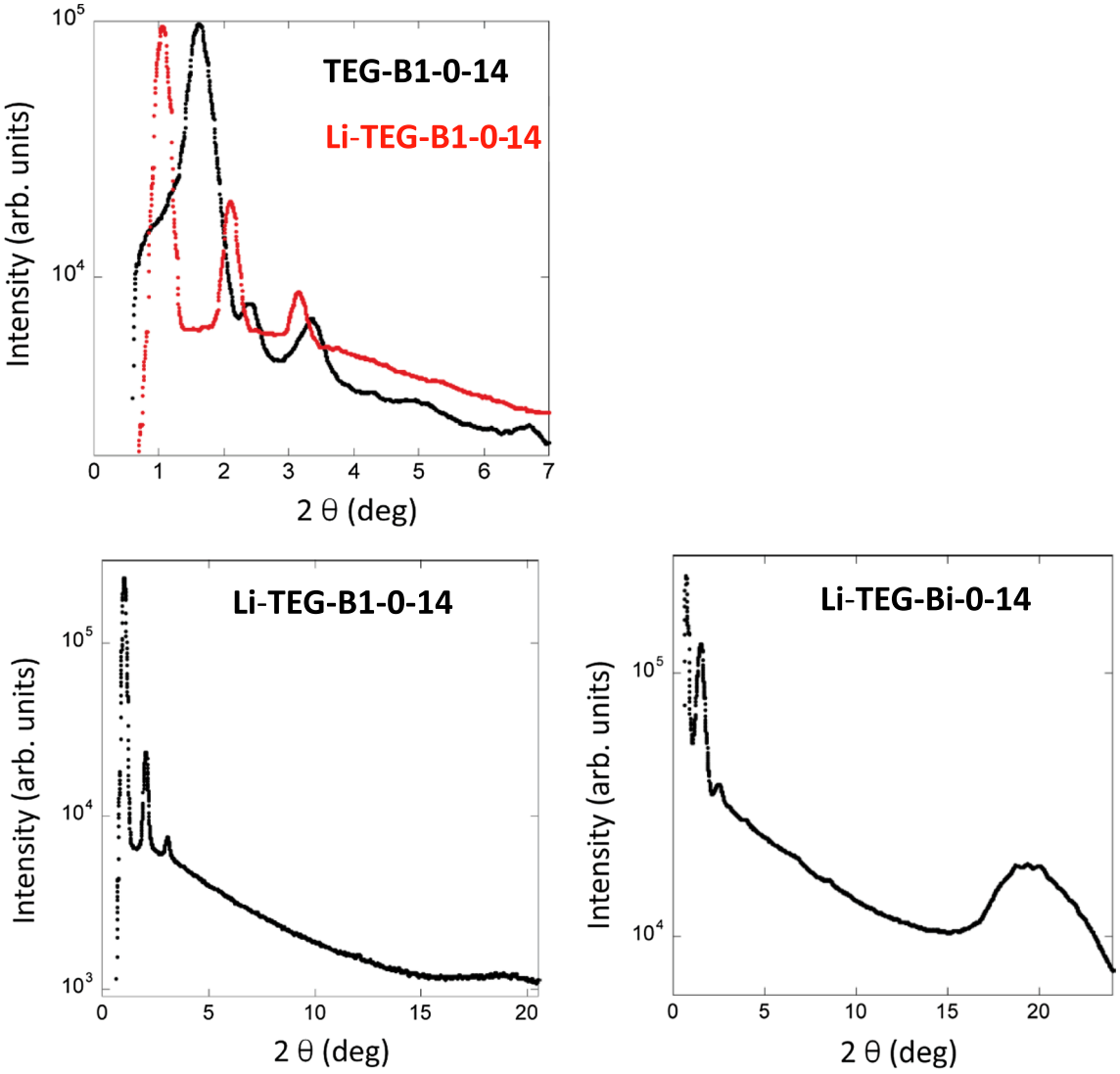

Fig. 2. (top) Small-angle region of the XRD of **TEG-B1-0-14** (black line) and **Li-TEG-B1-0-14** (red line) at 80 °C. A larger lamellar periodicity for the Li-doped compound is evident. (bottom) XRD of **Li-TEG-B1-0-14** at 80 °C, and of **Li-TEG-Bi-0-14** at 60 °C, after cooling from the isotropic phase. The wide-angle region shows simply a diffuse halo for **Li-TEG-B1-0-14.** However, for **Li-TEG-Bi-0-14** a more complex *(hk0)* reflections is clearly visible.

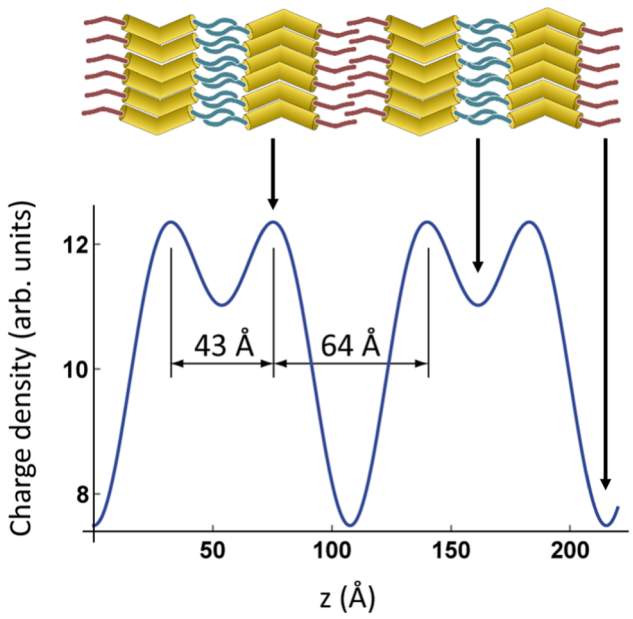

Fig. 3. Charge density map of **Li-TEG-Bazo-0-14** at room temperature. Yellow, blue and red regions in the scheme above represent the aromatic BC structure, the TEG chains and the alkyl tails respectively. Distances revealing the bilayer character of the structure are indicated. z is the coordinate along the smectic layer normal.

bilayers formed by two BC mesogens in a head-to-head disposition. The core distance through the EO sublayers are around 23 Å, 28 Å and 43 Å for **Li-TEG-B1-0-14**, **Li-TEG-Bi-0-14** and **Li-TEG-Bazo-0-14**, respectively. These values are much smaller than the above-mentioned estimated molecular lengths and suggest a strong intercalation of the flexible EO chains in the mesophase. On the other hand, the core-to-core distances though the aliphatic chains are 57 Å, 63 Å and 64 Å for **Li-TEG-B1-0-14**, **Li-TEG-Bi-0-14** and **Li-TEG-Bazo-0-14**, respectively. This indicates that intercalation of the alkyl chains is only significant for **Li-TEG-B1-0-14,** in good agreement with the reported differences from SmCP *vs* HNF organizations. [48,50] According to this, the difference between the experimental lamellar distance and the estimated length of the bilayer can be explained as a certain degree of intercalation of the flexible chains. However, some contribution from a possible tilt of the bent-core systems cannot be ruled out.

2.2.2. *Gel self-assemblies of bent-core amphiphiles*

The gelation properties of the compounds **TEG-Bx-0-14** and their Li-doped materials **Li-TEG-Bx-0-14** were assessed in solvents of different nature and polarity. For this purpose, initially 1% wt mixtures of these bent-core based solids and the selected solvent were heated to a temperature 5 °C below the boiling point of the liquid and left to cool to room temperature. Then, a *vial inversion test* was carried out to check the gelation properties of the materials. While liquids such as toluene, dioxane and DMF solve all these solids, they were insoluble in water and ethanol. In contrast, all pure amphiphiles **TEG-Bx-0-14** and hybrid materials **Li-TEG-Bx-0-14** were able to form gels in 1-octanol. Additionally, stable gels in n-dodecane are formed in the case of **TEG-Bx-0-14**, showing the good tendency of these materials to form gels in these non-polar solvents. Furthermore, prospective concentration studies were performed with **TEG-B1-0-14** in 1-octanol, demonstrating that stable gels are formed from 0.2% wt to 2% wt (Fig. 4**a)** revealing its supergelator character. According to this, it is reasonable to think that in the gel state the molecules of solvent may establish strong interactions with the hydrocarbon-chains of the bent-core amphiphiles.

TEM experiments were performed in order to study the morphology of the three-dimensional network of these organogels. A selection of the pictures is shown in Figs. 5-7. All the gelators self-assemble into fibrillar nanostructures of few nanometres in width and several microns in

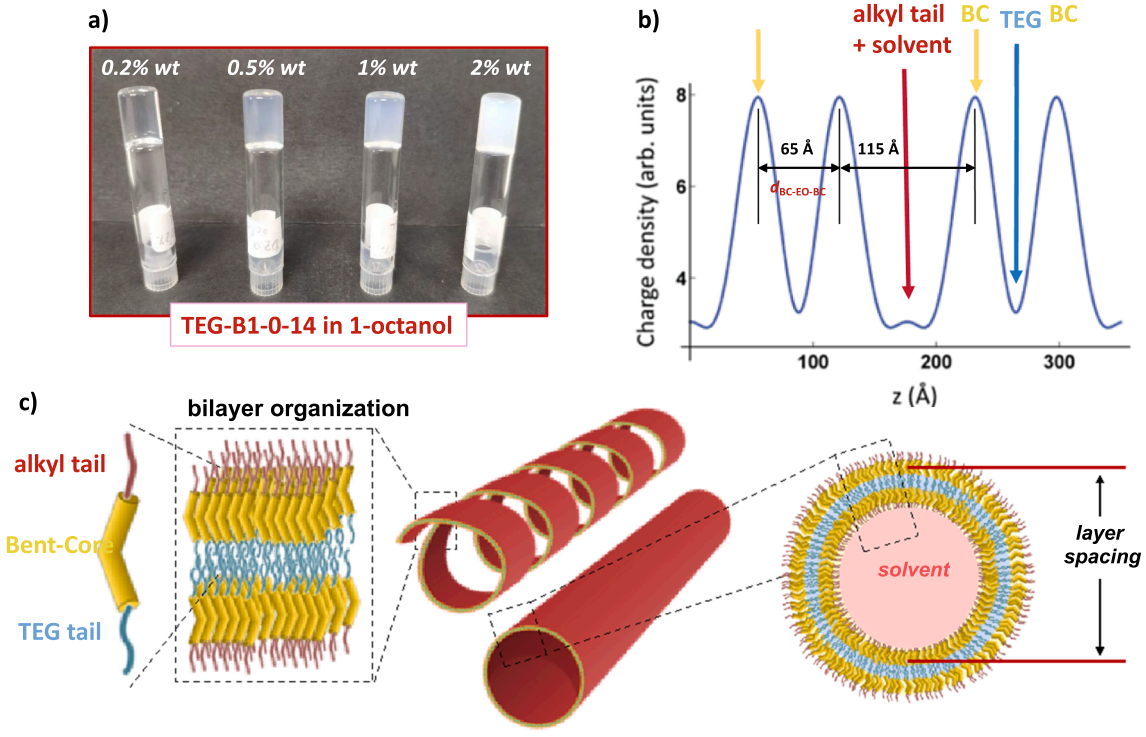

Fig. 4. a) Photography of the inverted vials with gels of **TEG-B1-0-14** at 0.2% wt, 0.5% wt, 1% wt and 2% wt in 1-octanol. b) XRD estimated charge density map for the gel of **TEG-B1-0-14** at 1% wt in 1-octanol. Maxima and minima are associated with the different parts of the molecule and the presence of solvent. z is the coordinate along the lamellar layer normal. c) Schematic representation of the bilayer organization of the amphiphilic BC molecules proposed for the helical fibers and hollow tubes that constitute the network of organogels based on **TEG-Bx-0-14** amphiphiles or on hybrid materials **Li-TEG-Bx-0-14**.

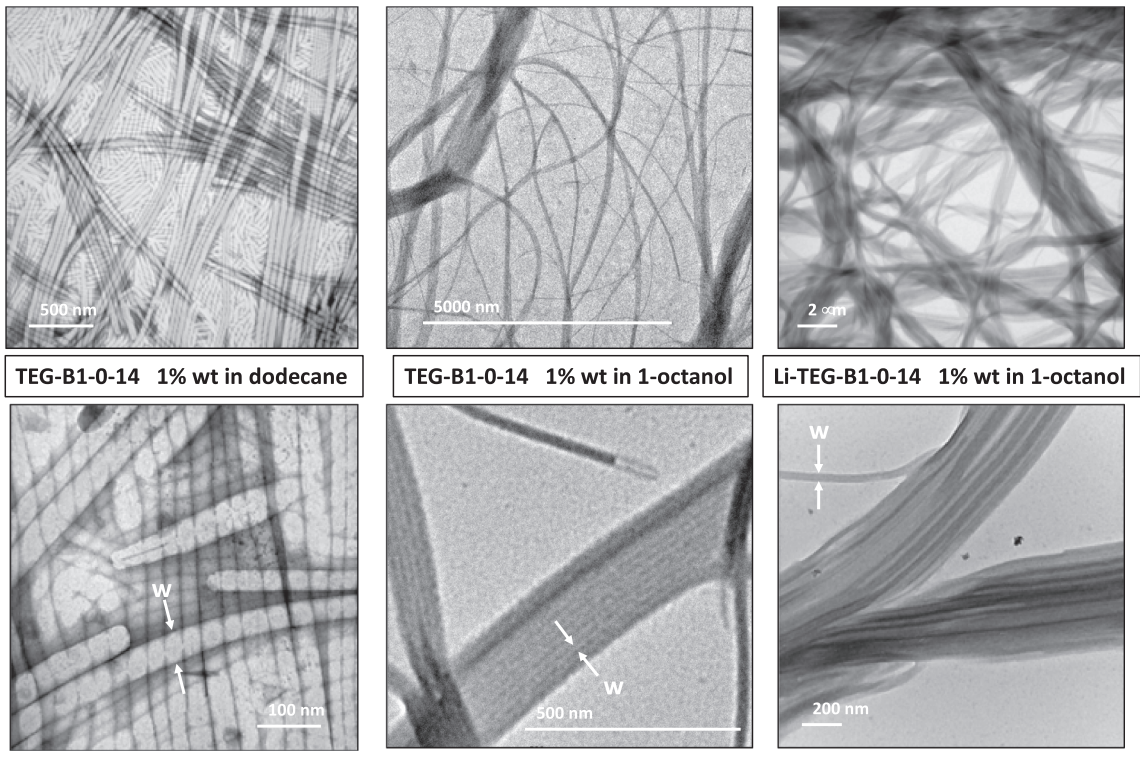

Fig. 5. TEM pictures of the gels of **TEG-B1-0-14** at 1% wt in dodecane and in 1-octanol, and of **Li-TEG-B1-0-14** at 1% wt in 1-octanol. The width of some of the fibers is indicated by w.

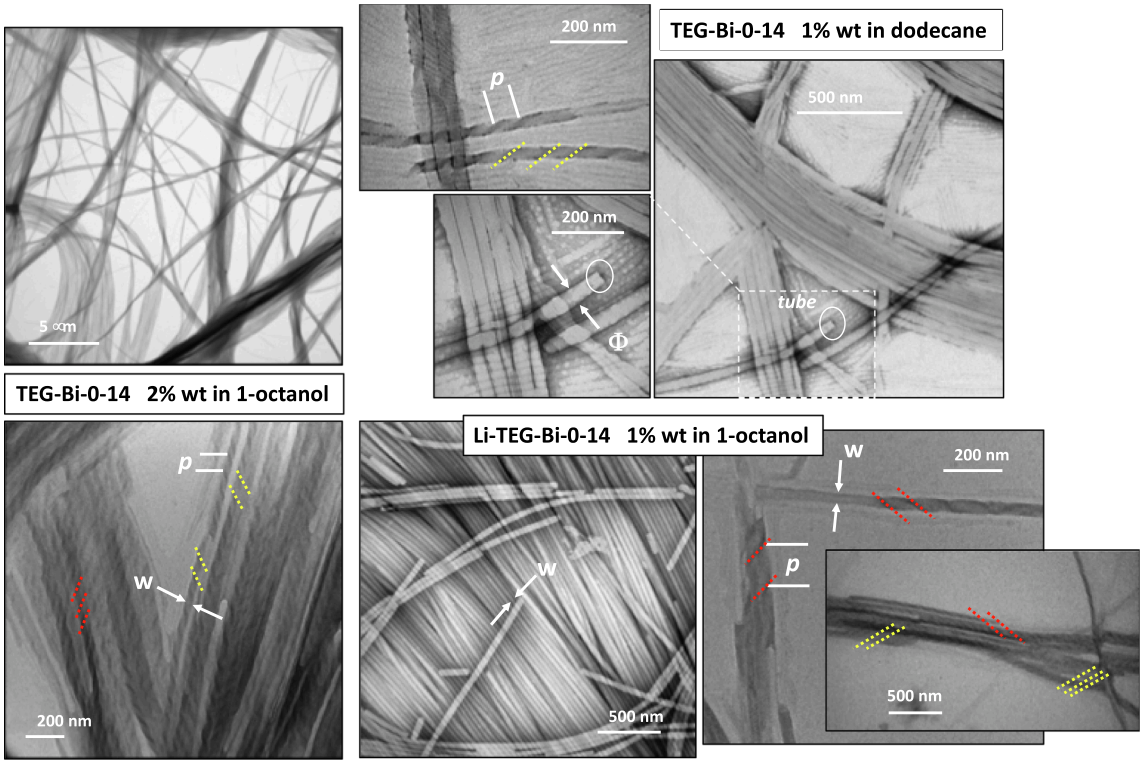

Fig. 6. TEM pictures of the gels of **TEG-Bi-0-14** at 1% wt in n-dodecane and at 2% wt in 1-octanol, and of **Li-TEG-Bi-0-14** at 1% wt in 1-octanol. The yellow and red lines indicate the left- and right-handed helical arrangements, respectively, with pitch *p*. The width of some of the fibers and the diameter of some of the tubes are indicated by w and Φ respectively.

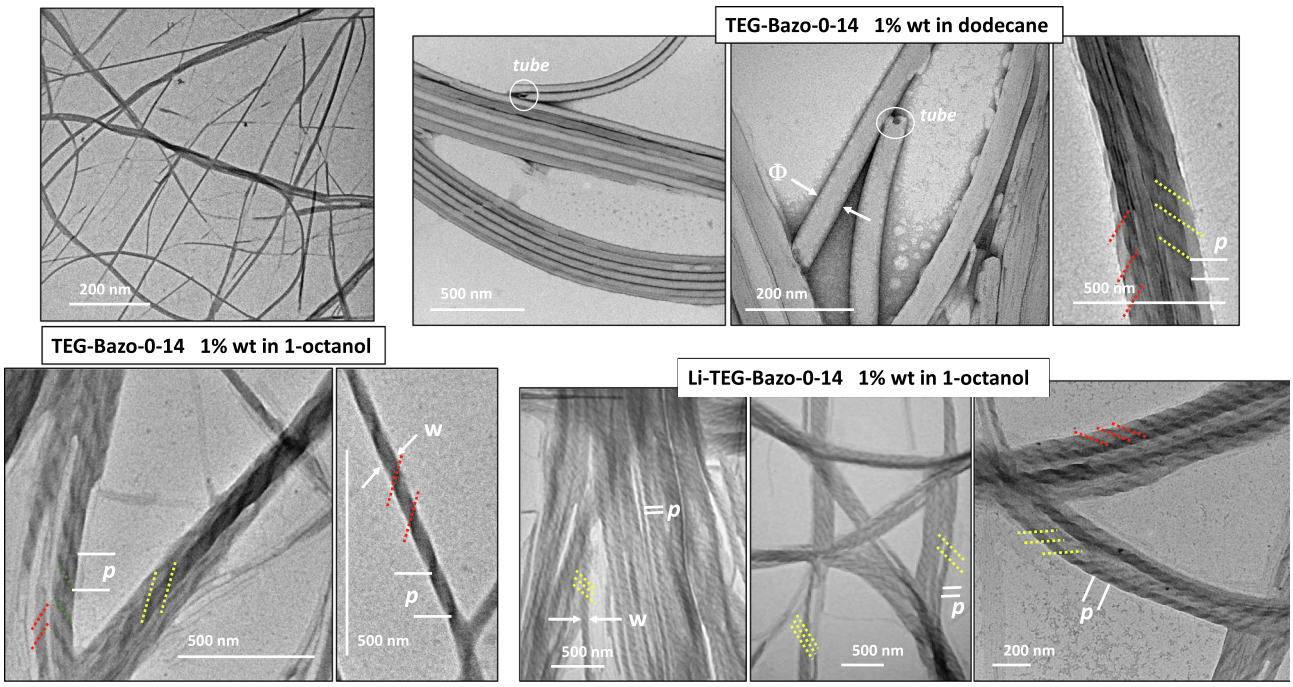

Fig. 7. TEM pictures of the gels of **TEG-Bazo-0-14** at 1% wt in n-dodecane and in 1-octanol, and of **Li-TEG-Bi-0-14** at 1% wt in 1-octanol. The yellow and red lines indicate the left- and right-handed helical arrangements, respectively, with pitch *p*. The width of some of the fibers and the diameter of some of the tubes are indicated by w and Φ respectively.

Table 2
Morphology and dimensions of the three-dimensional network of the gels of the TEG-based BC compounds and the lithium-doped materials. [w: width of fibers; L: length of fibers, Φ: diameter of nanotubes; *p*: pitch of twisted fibers. a) Measured from TEM pictures. b) Calculated from XRD patterns. C) Bent-core/Bent-core distance through EO tails calculated from XRD patterns].

Material		Morphology	Dimensions [a]	Layer spacing [b]	$d_{BC\text{-}EO\text{-}BC}$ [c]
Compound	**Solvent**				
TEG-B1-0-14	n-dodecane	tubular nanofibers	L: several μm w or Φ: 30-60 nm	–	–
	1-octanol	nanofibres	L: several μm w: 20-30 nm	180 Å	65 Å
Li-TEG-B1-0-14	1-octanol	nanofibres	L: several μm w: 40-60 nm	180 Å	60 Å
TEG-Bi-0-14	n-dodecane	helical nanofibres and tubular nanofibers	L: several μm w: 40-50 nm *p*: 60-80 nm Φ: 30-50 nm	280 Å	65 Å
	1-octanol	helical nanofibres	L: several μm w: 30-50 nm *p*: 100-110 nm	270 Å	80 Å
Li-TEG-Bi-0-14	1-octanol	helical nanofibres	L: several μm w: 30-50 nm *p*: 70-100 nm	290 Å	85 Å
TEG-Bazo-0-14	n-dodecane	helical nanofibres and tubular nanofibers	L: several μm w: 60 nm *p*: 60-120 nm Φ: 50-60 nm	300 Å	65 Å
	1-octanol	helical nanofibres	L: several μm w: 40-50 nm *p*: 100-110 nm	290 Å	75 Å
Li-TEG-Bazo-0-14	1-octanol	helical nanofibres	L: several μm w: 40-50 nm *p*: 60-90 nm	300 Å	85 Å

length (Table 2).

In n-dodecane, the gel of **TEG-B1-0-14** is formed by long fibers as shown from TEM pictures (Fig. 5) that could be identified as a tubular morphology. Additionally, the gels of **TEG-B1-0-14** and **Li-TEG-B1-0-14** in 1-octanol show fibrillar aggregates that formed a dense network (Fig. 5). In both cases, the BC amphiphiles self-assembled in flat nanofibres with widths ranging from 20 to 60 nm. No remarkable differences between the gels of **TEG-B1-0-14** and **Li-TEG-B1-0-14** in 1-octanol were observed, suggesting that, unlike in the case of the liquid-crystalline properties, the presence of lithium cations do not significantly affect the gelation properties of the molecules.

On the other hand, gels in 1-octanol based on molecules containing both the Bi- and Bazo-based lateral structures, **TEG-Bi-0-14**, **Li-TEG-Bi-0-14**, **TEG-Bazo-0-14** and **Li-TEG-Bazo-0-14,** revealed the formation of right and left-handed helical fibres, once again with no remarkable differences between the gels without or with lithium-doping **(**Figs. 6 and 7**).** The dimensions of the fibres, from 30 to 60 nm in width and helical pitches ranging from 60 to 120 nm, are in good agreement with those reported for the helical nanofilaments in other liquid-crystalline phases [50,73] and also similar to the values described for helical and twisted-shaped arrangements in solvent of other BC molecules previously reported. [65,89,96–98] This observation, together with the fact that both **Li-TEG-Bi-0-14** and **Li-TEG-Bazo-0-14** favour HNF-like mesophase organizations, lead us to think that the wound fibrillar network of the corresponding gels is composed of HNF-like fibres surrounded by solvent molecules. [96,98].

Moving on to the gels of **TEG-Bi-0-14** and **TEG-Bazo-0-14** in n-dodecane **(**Figs. 6 and 7**),** two different types of fibrillar assemblies were clearly observed in TEM pictures: helical filaments and tubules. While the former show helicity of both handedness, no evidence of supramolecular chirality was associated to the nanotubes, in contrast to the case of other compounds, including BC-molecules reported in the literature [8,89] **(**Figs. 6 and 7**).**

XRD experiments for gels were performed in order to study the molecular disposition within the fibrillar networks (Fig. 8**, S11, S12 and S13**). As a general rule, no significant differences were observed

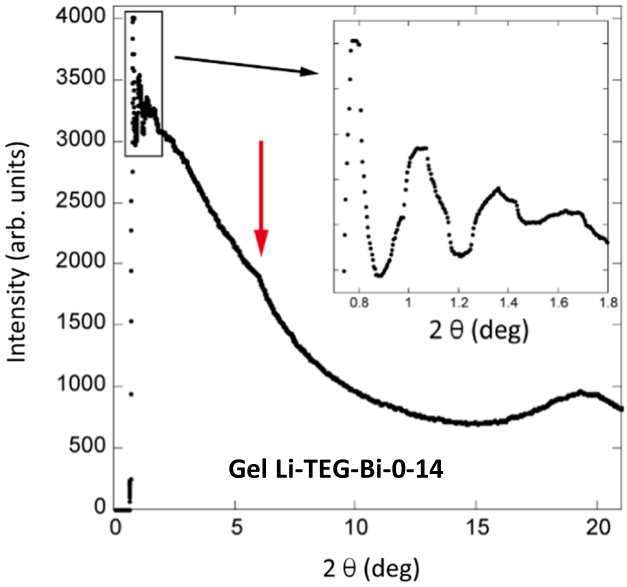

Fig. 8. XRD pattern for 1% wt gel of **Li-TEG-Bi-0-14** in 1-octanol. Two broad reflections at about 6° (red arrow) and 19° connected with the dimensions of the solvent molecule are observed. At the small-angle region, enlarged in the inset, a series of periodic peaks appear, which correspond to a layer structure of the gel.

between the gels derived from gelators **TEG-Bx-0-14** and those from Li-doped materials, showing that in these soft materials the influence of the lithium cations on the nanostructured organizations is less relevant that in the neat materials.

Depending on the solvent used, the XRD reflections of the gels had superimposed intense broad peaks at different angles, which were indicative of some characteristic sizes of the solvent molecules. Thus, for gels based on 1-octanol an intense peak was observed at around 19º, which corresponds to the width of the solvent molecules (Fig. 8). This signal overlaps with the diffuse halo and prevents the assignment of the (*hk*0) reflections observed in some of the mesophases. Another less intense diffuse peak at around 6º was also observed, which is related to the length of the molecules of 1-octanol. In the gels with n-dodecane some peaks at angles characteristic of the size of the solvent molecules were also observed (**Figure S13**). Some of those reflections take place in the wide-angle region, also hiding any information about the gel from reflections in this angular range.

The relevant information for the gels is found in the small angle zone. That region was studied separately with measurements carried out with an x-ray goniometer specific for low angles, given the large characteristic distances involved in these materials (**Figures S11 and S12**). In all gels XRD patterns showed a series of periodic peaks corresponding to a layered disposition of the BC molecules. In some samples, the reflections reached up to the fifth harmonic as in the gel of **TEG-Bazo-0-14** in 1-octanol (**Figure S11**), which indicates that the layers present a non-trivial internal structure. The layer spacings calculated from this data are summarized in Table 2 revealing spacings much larger than those previously obtained for the same materials in the mesophase. This means that there is a great intercalation of the solvent molecules within the layer structure. To analyze the lamellar structure we undertook studies of electronic density, which was deduced from the intensities of (00*l*) peaks (see the details of the procedure followed in the SI). [95] In all cases the density curves allowed to identify the segregation of the three parts of the gelator, i.e., the BC units, the EO tails, and the aliphatic chains together with the molecules of solvent. Fig. 4**b** shows a representative example for the gel **TEG-B1-0-14** in 1-octanol in which the three regions were easily identified. As pointed out, the incorporation of solvent molecules in the aliphatic chain region is necessary to explain the large size of the small-density region deduced, which is always much larger than twice the length of the chains. This is especially noticeable for the cases with the largest lamellar spacing, because the core-to-core distance through the EO sublayers ($d_{\mathbf{BC\text{-}EO\text{-}BC}}$) is roughly similar in all the cases, as shown in Table 2.

At first glance, these results would seem to indicate that there is a remarkable correlation between layers formed by two BC units through a very thick layer formed essentially by solvent molecules. It should be noted however that the experimental data do not necessarily lead to this conclusion. Indeed, in the small-angle diffractometer used in our measurements, the correlation length ξ (obtained from the width of the Bragg peaks Δθ of a standard crystalline sample, $\xi \approx \lambda/\Delta\theta$ is around 400 Å (λ is the x-ray wavelength)). [99] Although ξ is large enough in most situations of practical interest, it only represents a pair of smectic planes in our case. In other words, the resolution of the diffractometer does not allow to determine if there are more than two repeating units in some of the measurements. Then, the structure might actually be composed by only two repeating units in some cases. Therefore, considering the width w and diameter Φ dimensions estimated form TEM figures and gathered in Table 2, the conclusion could be that these repeating units are just the two walls of the hollow tube. The repetition distance is indicated in the right most diagram in Fig. 4c. Then we would simply have structures (hollow tube or helical fibers) in which the walls are formed by the two BCs joined by the chains of EO, with the alkyl tails facing to the hydrocarbon-based solvents. Thus, the inside and outside of the tube or helical fibers would consist of aliphatic chains and solvent molecules (see Fig. 4). In this way, the very long core-to-core distances through the aliphatic chains would simply contribute to the diameter of the tubular or of the helical fibers. Other possibilities of self-assembly involving several smectic layers in the usual way can also be operative to give rise to the fibers. [89,98] Presumably the wound morphology in some gels (e.g. **TEG-Bi-0-14**, **Li-TEG-Bi-0-14**, **TEG-Bazo-0-14** and **Li-TEG-Bazo-0-14**) is inherited from that of **Li-TEG-Bi-0-14** and **Li-TEG-Bazo-0-14** displaying HNF-type phases.

3. Conclusions

The liquid crystalline phases and organogels, of three new BC amphiphilic molecules **[TEG-Bx-0-14]** which incorporate a short polar TEG moiety directly grafted to the rigid-core are reported. In addition, their [1/1] lithium ion containing materials **[Li-TEG-Bx-0-14]** are also studied.

Interestingly, while none of the TEG-bent core amphiphiles induce liquid crystal assemblies, all the Li-doped materials were able to stabilize BC mesophases (SmCP or HNF). In the case of **Li-TEG-Bi-0-14** the mesophase even appears at room temperature. Alternatively, all these compounds, even at very low concentrations, form organogels of non-polar solvents such as 1-octanol and n-dodecane. Depending on both the gelator and the solvent, the morphology of the three-dimensional network of the gels provide highly demanded supramolecular nanostructures, from platelet or helical-fibers to tubules.

These studies demonstrate that TEG-decorated BC compounds are suitable amphiphiles for functional supramolecular materials chemistry, not only in bulk but also in solvents. Besides, EO-based BC amphiphiles provide a facile route to prepare nanostructured soft-materials. The self-assembly of non-chiral BC molecules gives rise to conformational chirality, which can be transferred to different nanostructures, even in the presence of lithium cations. Furthermore, by a subtle balance between molecule/solvent interactions the morphology of the aggregations can be regulated.

These novel findings contribute to the understanding of supramolecular self-aggregation process of BC amphiphiles, and will surely help to a better comprehension on how and why symmetry breaking occurs in this type of systems. Moreover, these compounds can be used towards appealing soft-materials, with potentials in various applications such as soft-electrolytes and chiral recognition or sensing. These are the subjects

of our current research projects, including photo-processes for azobenzene-based soft-materials.

CRediT authorship contribution statement

Martín Castillo-Vallés: Investigation, Methodology. **César L. Folcia:** Investigation. **Josu Ortega:** Investigation. **Jesús Etxebarria:** Investigation. **M. Blanca Ros:** Conceptualization, Funding acquisition.

Declaration of Competing Interest

The authors declare that they have no known competing financial interests or personal relationships that could have appeared to influence the work reported in this paper.

Data availability

No data was used for the research described in the article.

Acknowledgements

The authors from INMA greatly appreciate the Spanish Government projects, PGC2018-093761-B-C31 [MCIU/AEI/FEDER, UE] and PID2021-122882NB-I00 funded by MCIN/AEI /10.13039/501100011033/ y by FEDER *Una manera de hacer Europa;* the Gobierno de Aragón/FEDER (research group E47_20R), the Basque Government (Project IT1458-22), and BES-2016-078753 MINECO-FEDER (M. C.-V.) fellowship programs for support. Authors would like to acknowledge the nuclear magnetic resonance, mass spectrometry, and thermal analysis services of CEQMA (Univ. Zaragoza-CSIC), the LMA (Univ. Zaragoza) for TEM equipment and the use of Servicio General de Apoyo a la Investigación-SAI, Universidad de Zaragoza.

Appendix A. Supplementary data

Supplementary data to this article can be found online at https://doi.org/10.1016/j.molliq.2023.121825.

References

[1] J. Hulvat, M. Sofos, Self-Assembly and Luminescence of Oligo (p-Phenylene Vinylene) Amphiphiles, J. Am. Chem. Soc. 127 (11) (2005) 366–372.
[2] S. Shin, S.H. Gihm, C.R. Park, S. Kim, S.Y. Park, Water-Soluble Fluorinated and PEGylated Cyanostilbene Derivative: An Amphiphilic Building Block Forming Self-Assembled Organic Nanorods with Enhanced Fluorescence Emission, Chem. Mater. 25 (16) (2013) 3288–3295.
[3] A. Pipertzis, G. Zardalidis, K. Wunderlich, M. Klapper, K. Müllen, G. Floudas, Ionic Conduction in Poly(Ethylene Glycol)-Functionalized Hexa-Peri-Hexabenzocoronene Amphiphiles, Macromolecules 50 (5) (2017) 1981–1990.
[4] S. Yu, Y. Yang, T. Chen, J. Xu, L.Y. Jin, Donor-Acceptor Interaction-Driven Self-Assembly of Amphiphilic Rod-Coil Molecules into Supramolecular Nanoassemblies, Nanoscale 9 (45) (2017) 17975–17982.
[5] Y. Chang, Y. Jiao, H.E. Symons, J.F. Xu, C.F.J. Faul, X. Zhang, Molecular Engineering of Polymeric Supra-Amphiphiles, Chem. Soc. Rev. 48 (4) (2019) 989–1003.
[6] J. Dey, R. Ghosh, R. Das Mahapatra, Self-Assembly of Unconventional Low-Molecular-Mass Amphiphiles Containing a PEG Chain, Langmuir 35 (4) (2019) 848–861.
[7] A. Sikder, S. Ghosh, Hydrogen-Bonding Regulated Assembly of Molecular and Macromolecular Amphiphiles, Mater. Chem. Front. 3 (12) (2019) 2602–2616.
[8] Y. Cui, D. Tao, X. Huang, G. Lu, C. Feng, Self-Assembled Helical and Twisted Nanostructures of a Preferred Handedness from Achiral π-Conjugated Oligo(p-Phenylenevinylene) Derivatives, Langmuir 35 (8) (2019) 3134–3142.
[9] M. Sun, M. Lee, Switchable Aromatic Nanopore Structures: Functions and Applications, Acc. Chem. Res. 54 (14) (2021) 2959–2968.
[10] J. Cui, K. Zhao, M. Li, P. Zhang, Sticktight-Inspired PEGylation for Low-Fouling Coatings, Chem. Commun. 13735–13738 (2022).
[11] B.K. Cho, Nanostructured Organic Electrolytes, RSC Adv. 4 (1) (2014) 395–405.
[12] Z. Xue, D. He, X. Xie, Poly(Ethylene Oxide)-Based Electrolytes for Lithium-Ion Batteries, J. Mater. Chem. A 3 (38) (2015) 19218–19253.
[13] T.S. Dörr, A. Pelz, P. Zhang, T. Kraus, M. Winter, H.D. Wiemhöfer, An Ambient Temperature Electrolyte with Superior Lithium Ion Conductivity Based on a Self-Assembled Block Copolymer, Chem. - A Eur. J. 24 (32) (2018) 8061–8065.
[14] S. Venkatesan, I.P. Liu, J.C. Lin, M.H. Tsai, H. Teng, Y.L. Lee, Highly Efficient Quasi-Solid-State Dye-Sensitized Solar Cells Using Polyethylene Oxide (PEO) and Poly(Methyl Methacrylate) (PMMA)-Based Printable Electrolytes, J. Mater. Chem. A 6 (21) (2018) 10085–10094.
[15] G. Zhang, Y.L. Hong, Y. Nishiyama, S. Bai, S. Kitagawa, S. Horike, Accumulation of Glassy Poly(Ethylene Oxide) Anchored in a Covalent Organic Framework as a Solid-State Li + Electrolyte, J. Am. Chem. Soc. 141 (3) (2019) 1227–1234.
[16] M. Yoshitake, J. Han, T. Sakai, M. Morita, K. Fujii, TetraPEG Network Formation via a Michael Addition Reaction in an Ionic Liquid: Application to Polymer Gel Electrolyte for Electric Double-Layer Capacitors, Chem. Lett. 48 (7) (2019) 704–707.
[17] T.N.T. Phan, S. Issa, D. Gigmes, Poly(Ethylene Oxide)-Based Block Copolymer Electrolytes for Lithium Metal Batteries, Polym. Int. 68 (1) (2019) 7–13.
[18] G. Song, H. Bin Son, D.Y. Han, M. Je, S. Nam, S. Park, A Renewable Future: A Comprehensive Perspective from Materials to Systems for next-Generation Batteries, Mater. Chem. Front. 5 (8) (2021) 3344–3377.
[19] M.S.A. Rani, N.A. Abdullah, M.H. Sainorudin, M. Mohammad, S. Ibrahim, The Development of Poly(Ethylene Oxide) Reinforced with a Nanocellulose-Based Nanocomposite Polymer Electrolyte in Dye-Sensitized Solar Cells, Mater. Adv. 2 (16) (2021) 5465–5470.
[20] S. Tang, W. Guo, Y. Fu, Advances in Composite Polymer Electrolytes for Lithium Batteries and Beyond, Adv. Energy Mater. 11 (2) (2021) 2000802.
[21] W. Huang, J. Chen, G. Wang, Y. Yao, X. Zhuang, R.M. Pankow, Y. Cheng, T. J. Marks, A. Facchetti, Dielectric Materials for Electrolyte Gated Transistor Applications, J. Mater. Chem. C 9 (30) (2021) 9348–9376.
[22] J.W. Suen, N.K. Elumalai, S. Debnath, N.M. Mubarak, C.I. Lim, M.M. Reddy, The Role of Interfaces in Ionic Liquid-Based Hybrid Materials (Ionogels) for Sensing and Energy Applications, *Adv. Mater*, Interfaces 9 (2022) 2201405.
[23] R. Xue, Y. Han, Y. Xiao, J. Huang, B.Z. Tang, Y. Yan, Lithium Ion Nanocarriers Self-Assembled from Amphiphiles with Aggregation-Induced Emission Activity, ACS Appl. Nano Mater. 1 (1) (2018) 122–131.
[24] N. Kameta, J. Dong, H. Yui, Thermoresponsive PEG-Coated Nanotubes as Chiral Selectors of Amino Acids and Peptides, Small 14 (15) (2018) 1800030.
[25] V. Bhushan, M.P. Heitz, G.A. Baker, S. Pandey, Ionic Liquid-Controlled Shape Transformation of Spherical to Nonspherical Polymersomes via Hierarchical Self-Assembly of a Diblock Copolymer, Langmuir 37 (16) (2021) 5081–5088.
[26] W. Liu, A. Wang, R. Yang, H. Wu, S. Shao, J. Chen, Y. Ma, Z. Li, Y. Wang, X. He, et al., Water-Triggered Stiffening of Shape-Memory Polyurethanes Composed of Hard Backbone Dangling PEG Soft Segments, Adv. Mater. 2201914 (2022) 1–9.
[27] J. Chen, A. Rizvi, J.P. Patterson, C.J. Hawker, Discrete Libraries of Amphiphilic Poly(Ethylene Glycol) Graft Copolymers: Synthesis, Assembly, and Bioactivity, J. Am. Chem. Soc. 144 (42) (2022) 19466–19474.
[28] H. Hu, M. Gopinadhan, C.O. Osuji, Directed Self-Assembly of Block Copolymers: A Tutorial Review of Strategies for Enabling Nanotechnology with Soft Matter, Soft Matter 10 (22) (2014) 3867–3889.
[29] N. Aljuaid, M. Tully, J. Seitsonen, J. Ruokolainen, I.W. Hamley, Benzene Tricarboxamide Derivatives with Lipid and Ethylene Glycol Chains Self-Assemble into Distinct Nanostructures Driven by Molecular Packing, Chem. Commun. 57 (67) (2021) 8360–8363.
[30] Z. Xu, W. Li, Control the Self-Assembly of Block Copolymers by Tailoring the Packing Frustration, Chinese J. Chem. 40 (9) (2022) 1083–1090.
[31] B. Jin, Y. Chen, Y. Luo, X. Li, Precise and Controllable Assembly of Block Copolymers, Chinese J. Chem. 41 (2023) 93–110.
[32] Z. Lu, K. Zhong, Y. Liu, Z. Li, T. Chen, L.Y. Jin, Self-Organizing: P -Quinquephenyl Building Blocks Incorporating Lateral Hydroxyl and Methoxyl Groups into Supramolecular Nano-Assemblies, Soft Matter 12 (17) (2016) 3860–3867.
[33] T. Kato, M. Yoshio, T. Ichikawa, B. Soberats, H. Ohno, M. Funahashi, Transport of Ions and Electrons in Nanostructured Liquid Crystals, Nat. Rev. Mater. 2 (4) (2017) 17001.
[34] T. Kato, J. Uchida, T. Ichikawa, T. Sakamoto, Functional Liquid Crystals towards the Next Generation of Materials, Angew. Chemie - Int. Ed. 57 (16) (2018) 4355–4371.
[35] N. Kameta, H. Shiroishi, PEG-Nanotube Liquid Crystals as Templates for Construction of Surfactant-Free Gold Nanorods, Chem. Commun. 54 (37) (2018) 4665–4668.
[36] T. Kato, M. Gupta, D. Yamaguchi, K.P. Gan, M. Nakayama, Supramolecular Association and Nanostructure Formation of Liquid Crystals and Polymers for New Functional Materials, Bull. Chem. Soc. Jpn. 94 (1) (2021) 357–376.
[37] J. Uchida, B. Soberats, M. Gupta, T. Kato, Advanced Functional Liquid Crystals, Adv. Mater. 34 (23) (2022) 1–33.
[38] N. Kapernaum, A. Lange, M. Ebert, M.A. Grunwald, C. Haege, S. Marino, A. Zens, A. Taubert, F. Giesselmann, S. Laschat, Current Topics in Ionic Liquid Crystals John Wiley and Sons Inc January 1 ChemPlusChem. 87 (2022) e202100397.
[39] E. Gorecka, N. Vaupotič, A. Zep, D. Pociecha, From Sponges to Nanotubes: A Change of Nanocrystal Morphology for Acute-Angle Bent-Core Molecules, Angew. Chemie - Int. Ed. 55 (40) (2016) 12238–12242.
[40] C. Nilsson, J. Østergaard, S.W. Larsen, C. Larsen, A. Urtti, A. Yaghmur, PEGylation of Phytantriol-Based Lyotropic Liquid Crystalline Particles-the Effect of Lipid Composition, PEG Chain Length, and Temperature on the Internal Nanostructure, Langmuir 30 (22) (2014) 6398–6407.
[41] V. Pérez-Gregorio, M. Cano, I. Gascón, N. Gimeno, M.B. Ros, M. Carmen López, Study of an Ethylene Oxide-Terminated Bent-Core Compound: Synthesis and Langmuir-Blodgett Film Structure, J. Colloid Interface Sci. 406 (2013) 60–68.
[42] X. Liu, H. Li, Y. Kim, M. Lee, Assembly-Disassembly Switching of Self-Sorted Nanotubules Forming Dynamic 2-D Porous Heterostructure, Chem. Commun. 54 (25) (2018) 3102–3105.

[43] M. Castillo-Vallés, A. Martínez-Bueno, R. Giménez, T. Sierra, M.B. Ros, Beyond Liquid Crystals: New Research Trends for Mesogenic Molecules in Liquids, J. Mater. Chem. C 7 (46) (2019) 14454–14470.
[44] R.A. Reddy, C. Tschierske, Bent-Core Liquid Crystals: Polar Order, Superstructural Chirality and Spontaneous Desymmetrisation in Soft Matter Systems, J. Mater. Chem. 16 (10) (2006) 907–961.
[45] H. Takezoe, Y. Takanishi, Bent-Core Liquid Crystals: Their Mysterious and Attractive World, Japanese J. Appl. Physics, Part 1 Regul. Pap. Short Notes Rev. Pap. 45 (2A) (2006) 597–625.
[46] C. Tschierske, Development of Structural Complexity by Liquid-Crystal Self-Assembly, Angew. Chemie - Int. Ed. 52 (34) (2013) 8828–8878.
[47] A. Eremin, A. Jákli, Polar Bent-Shape Liquid Crystals - From Molecular Bend to Layer Splay and Chirality, Soft Matter 9 (3) (2013) 615–637.
[48] J.W. Goodby, P.J. Collings, T. Kato, C. Tschierske, H. Gleeson, P. Raynes (Eds.), **2014** Handbook of Liquid Crystals, Wiley-VCH, Weinheim. Chapters 3, 4, 5 and 8 are focussed on bent-core liquid crystals.
[49] C. Tschierske, G. Ungar, Mirror Symmetry Breaking by Chirality Synchronisation in Liquids and Liquid Crystals of Achiral Molecules, ChemPhysChem 17 (1) (2016) 9–26.
[50] H. Takezoe, A. Eremin, Bent-Shaped Liquid Crystals: Structures and Physical Properties, Taylor & Francis, Boca Ratón, 2017.
[51] C. Tschierske, D.J. Photinos, Biaxial Nematic Phases, J. Mater. Chem. 20 (21) (2010) 4263–4294.
[52] A. Jákli, Liquid Crystals of the Twenty-First Century – Nematic Phase of Bent-Core Molecules, Liq. Cryst. Rev. 1 (1) (2013) 65–82.
[53] H.F. Gleeson, S. Kaur, V. Görtz, A. Belaissaoui, S. Cowling, J.W. Goodby, The Nematic Phases of Bent-Core Liquid Crystals, ChemPhysChem 15 (7) (2014) 1251–1260.
[54] A. Jákli, O.D. Lavrentovich, J.V. Selinger, Physics of Liquid Crystals of Bent-Shaped Molecules, Rev. Mod. Phys. 90 (4) (2018) 45004.
[55] F. Vita, F.C. Adamo, O. Francescangeli, Polar Order in Bent-Core Nematics: An Overview, J. Mol. Liq. 267 (2018) 564–573.
[56] V. Borshch, Y.K. Kim, J. Xiang, M. Gao, A. Jákli, V.P. Panov, J.K. Vij, C.T. Imrie, M. G. Tamba, G.H. Mehl, et al., Nematic Twist-Bend Phase with Nanoscale Modulation of Molecular Orientation, Nat. Commun. 4 (2013) 1–8.
[57] R.J. Mandle, Designing Liquid-Crystalline Oligomers to Exhibit Twist-Bend Modulated Nematic Phases, Chem. Rec. 18 (9) (2018) 1341–1349.
[58] M. Nagaraj, Dark Conglomerate Phases of Bent-Core Liquid Crystals, Liq. Cryst. 43 (13–15) (2016) 2244–2253.
[59] K.V. Le, H. Takezoe, F. Araoka, Chiral Superstructure Mesophases of Achiral Bent-Shaped Molecules – Hierarchical Chirality Amplification and Physical Properties, Adv. Mater. 29 (25) (2017) 1–21.
[60] S. Kaur, V. Punjani, N. Yadav, A. Barthakur, A. Baghla, S. Dhara, S.K. Pal, Chemical and Physical Aspects of Recent Bent-Shaped Liquid Crystals Exhibiting Chiral and Achiral Mesophases, Liq. Cryst. 49 (7–9) (2022) 1078–1146.
[61] J. Etxebarria, M.B. Ros, Bent-Core Liquid Crystals in the Route to Functional Materials, J. Mater. Chem. 18 (25) (2008) 2919–2926.
[62] I.C. Pintre, J.L. Serrano, M.B. Ros, J. Martínez-Perdiguero, I. Alonso, J. Ortega, C. L. Folcia, J. Etxebarria, R. Alicante, B. Villacampa, Bent-Core Liquid Crystals in a Route to Efficient Organic Nonlinear Optical Materials, J. Mater. Chem. 20 (15) (2010) 2965–2971.
[63] H. Takezoe, Polar Liquid Crystals-Ferro, Antiferro, Banana, and Columnar, Mol. Cryst. Liq. Cryst. 646 (1) (2017) 46–65.
[64] K.I. Shivakumar, D. Pociecha, J. Szczytko, S. Kapuściński, H. Monobe, P. Kaszyński, Photoconductive Bent-Core Liquid Crystalline Radicals with a Paramagnetic Polar Switchable Phase, J. Mater. Chem. C 8 (3) (2020) 1083–1088.
[65] M. Martínez-Abadía, S. Varghese, J. Gierschner, R. Giménez, M.B. Ros, Luminescent Assemblies of Pyrene-Containing Bent-Core Mesogens: Liquid Crystals, π-Gels and Nanotubes, J. Mater. Chem. C 10 (33) (2022) 12012–12021.
[66] L.E. Hough, H.T. Jung, D. Krüerke, M.S. Heberling, M. Nakata, C.D. Jones, D. Chen, D.R. Link, J. Zasadzinski, G. Heppke, et al., Helical Nanofilament Phases, Science 325 (5939) (2009) 456–460.
[67] E. Tsai, J.M. Richardson, E. Korblova, M. Nakata, D. Chen, Y. Shen, R. Shao, N. A. Clark, D.M. Walba, A Modulated Helical Nanofilament Phase, Angew. Chemie - Int. Ed. 52 (20) (2013) 5254–5257.
[68] C. Zhang, N. Diorio, O.D. Lavrentovich, A. Jákli, Helical Nanofilaments of Bent-Core Liquid Crystals with a Second Twist, Nat. Commun. 5 (2014) 1–6.
[69] L. Li, M. Salamończyk, S. Shadpour, C. Zhu, A. Jákli, T. Hegmann, An Unusual Type of Polymorphism in a Liquid Crystal, Nat. Commun. 9 (1) (2018) 3–10.
[70] S. Shadpour, A. Nemati, N.J. Boyd, L. Li, M.E. Prévôt, S.L. Wakerlin, J.P. Vanegas, M. Salamończyk, E. Hegmann, C. Zhu, et al., Heliconical-Layered Nanocylinders (HLNCs)-Hierarchical Self-Assembly in a Unique B4 Phase Liquid Crystal Morphology, Mater. Horizons 6 (5) (2019) 959–968.
[71] S. Shadpour, A. Nemati, J. Liu, T. Hegmann, Directing the Handedness of Helical Nanofilaments Confined in Nanochannels Using Axially Chiral Binaphthyl Dopants, ACS Appl. Mater. Interfaces 12 (11) (2020) 13456–13463.
[72] W. Park, D.K. Yoon, Orientation Control of Helical Nanofilament Phase and Its Chiroptical Applications, Crystals 10 (8) (2020) 1–25.
[73] J. Liu, S. Shadpour, M.E. Prévôt, M. Chirgwin, A. Nemati, E. Hegmann, R. P. Lemieux, T. Hegmann, Molecular Conformation of Bent-Core Molecules Affected by Chiral Side Chains Dictates Polymorphism and Chirality in Organic Nano- And Microfilaments, ACS Nano 15 (4) (2021) 7249–7270.
[74] Y. Takanishi, F. Araoka, H. Iwayama, The Effect of the Structure of a Helical Nanofilament of the B4 Phase of Bent-Core Liquid Crystals on the Nano-Phase Separation Mixed with a Rod-like Cholesteric Liquid Crystal Mixture, RSC Adv. 12 (45) (2022) 29346–29349.
[75] F. Araoka, N.Y. Ha, Y. Kinoshita, B. Park, J.W. Wu, H. Takezoe, Twist-Gram-Boundary Structure in the B4 Phase of a Bent-Core Molecular System Identified by Second Harmonic Generation Circular Dichroism Measurement, Phys. Rev. Lett. 94 (13) (2005) 1–4.
[76] R.A. Callahan, D.C. Coffey, D. Chen, N.A. Clark, G. Rumbles, D.M. Walba, Charge Generation Measured for Fullerene-Helical Nanofilament Liquid Crystal Heterojunctions, ACS Appl. Mater. Interfaces 6 (7) (2014) 4823–4830.
[77] A. Zep, K. Sitkowska, D. Pociecha, E. Gorecka, Photoresponsive Helical Nanofilaments of B4 Phase, J. Mater. Chem. C 2 (13) (2014) 2323–2327.
[78] W. Park, T. Ha, T.T. Kim, A. Zep, H. Ahn, T.J. Shin, K.I. Sim, T.S. Jung, J.H. Kim, D. Pociecha, et al., Directed Self-Assembly of a Helical Nanofilament Liquid Crystal Phase for Use as Structural Color Reflectors, NPG Asia Mater 11 (1) (2019) 45.
[79] B.C. Kim, H.J. Choi, J.J. Lee, F. Araoka, S.W. Choi, Circularly Polarized Luminescence Induced by Chiral Super Nanospaces, Adv. Funct. Mater. 29 (35) (2019) 1–6.
[80] J.J. Lee, B.C. Kim, H.J. Choi, S. Bae, F. Araoka, S.W. Choi, Inverse Helical Nanofilament Networks Serving as a Chiral Nanotemplate, ACS Nano 14 (5) (2020) 5243–5250.
[81] T. Otani, F. Araoka, K. Ishikawa, H. Takezoe, Enhanced Optical Activity by Achiral Rod-like Molecules Nanosegregated in the B4 Structure of Achiral Bent-Core Molecules, J. Am. Chem. Soc. 131 (34) (2009) 12368–12372.
[82] S.W. Jeon, D.Y. Kim, F. Araoka, K.U. Jeong, S.W. Choi, Nanosegregated Chiral Materials with Self-Assembled Hierarchical Mesophases: Effect of Thermotropic and Photoinduced Polymorphism in Rodlike Molecules, Chem. - A Eur. J. 23 (70) (2017) 17794–17799.
[83] W. Lewandowski, N. Vaupotič, D. Pociecha, E. Górecka, L.M. Liz-Marzán, Chirality of Liquid Crystals Formed from Achiral Molecules Revealed by Resonant X-Ray Scattering, Adv. Mater. 32 (41) (2020) 1–17.
[84] K. Ariga, T. Mori, T. Kitao, T. Uemura, Supramolecular Chiral Nanoarchitectonics, Adv. Mater. 32 (41) (2020) 1–22.
[85] N. Gimeno, R. Martín-Rapún, S. Rodríguez-Conde, J.L. Serrano, C.L. Folcia, M. A. Pericás, M.B. Ros, "Click Chemistry" as a Versatile Route to Synthesize and Modulate Bent-Core Liquid Crystalline Materials, J. Mater. Chem. 22 (33) (2012) 16791–16800.
[86] Ń. Gimeno, J. Barbeŕa, J.L. Serrano, M.B. Ros, M.R. De La Fuente, I. Alonso, Ć. L. Folcia, Erminal Chains as a Tool to Modulate the Properties of Bent-Core Liquid Crystals, Chem. Mater. 21 (19) (2009) 4620–4630.
[87] V. Pérez-Gregorio, M. Cano, I. Gascón, N. Gimeno, M.B. Ros, M. Carmen López, Study of an Ethylene Oxide-Terminated Bent-Core Compound: Synthesis and Langmuir-Blodgett Film Structure, J. Colloid Interface Sci. 406 (2013) 60–68.
[88] W.-Z. Wang, C. Gao, Q. Zhang, X.-H. Ye, D.-H. Qu, Supramolecular Helical Nanofibers Formed by Achiral Monomers and Their Reversible Sol-Gel Transition, Chem. - An Asian J. 12 (4) (2017) 410–414.
[89] M. Castillo-Vallés, M. Cano, A. Bermejo-Sanz, N. Gimeno, M.B. Ros, Towards Supramolecular Nanostructured Materials: Control of the Self-Assembly of Ionic Bent-Core Amphiphiles, J. Mater. Chem. C 8 (6) (2020) 1998–2007.
[90] M. Alaasar, Azobenzene-Containing Bent-Core Liquid Crystals: An Overview, Liq. Cryst. 43 (13–15) (2016) 2208–2243.
[91] N. Begum, S. Kaur, G. Mohiuddin, R. Nandi, S.P. Gupta, N.V.S. Rao, S.K. Pal, Structural Understanding, Photoswitchability, and Supergelation of a New Class of Four Ring-Based Bent-Shaped Liquid Crystal, J. Phys. Chem. B 123 (20) (2019) 4443–4451.
[92] T. Shimizu, W. Ding, N. Kameta, Soft-Matter Nanotubes: A Platform for Diverse Functions and Applications, Chem. Rev. 120 (4) (2020) 2347–2407.
[93] X. Huang, R. Li, Z. Duan, F. Xu, H. Li, Supramolecular Polymer Gels: From Construction Methods to Functionality, Soft Matter 18 (20) (2022) 3828–3844.
[94] C. Zhu, J. Wu, J. Yan, X. Liu, Advanced Fiber Materials for Wearable Electronics, Adv. Fiber Mater. (2022). No. 0123456789.
[95] C.L. Folcia, I. Alonso, J. Ortega, J. Etxebarria, I. Pintre, M.B. Ros, Achiral Bent-Core Liquid Crystals with Azo and Azoxy Linkages: Structural and Nonlinear Optical Properties and Photoisomerization, Chem. Mater. 18 (19) (2006) 4617–4626.
[96] A. Zep, M. Salamonczyk, N. Vaupotic, D. Pociecha, E. Gorecka, Physical Gels Made of Liquid Crystalline B4 Phase, Chem. Commun. 49 (30) (2013) 3119–3121.
[97] W.Z. Wang, C. Gao, Q. Zhang, X.H. Ye, D.H. Qu, Supramolecular Helical Nanofibers Formed by Achiral Monomers and Their Reversible Sol–Gel Transition, Chem. - An Asian J. 12 (4) (2017) 410–414.
[98] J. Matraszek, N. Topnani, N. Vaupotič, H. Takezoe, J. Mieczkowski, D. Pociecha, E. Gorecka, Monolayer Filaments versus Multilayer Stacking of Bent-Core Molecules, Angew. Chemie - Int. Ed. 55 (10) (2016) 3468–3472.
[99] J. Ortega, C.L. Folcia, J. Etxebarria, J. Martínez-Perdiguero, J.A. Gallastegui, P. Ferrer, N. Gimeno, M. Blanca Ros, Electric-Field-Induced Phase Transitions in Bent-Core Mesogens Determined by x-Ray Diffraction, Phys. Rev. E - Stat. Nonlinear, Soft Matter Phys. 84 (2) (2011) 1–7.